



# Hygrothermal performance of a straw bale building: In situ and laboratory investigations



Omar Douzane\*, Geoffrey Promis, Jean-Marc Roucoult, Anh-Dung Tran Le, Thierry Langlet

Innovative Technologies Laboratory (LTI), University of Picardie Jules Verne, Avenue des Facultés, 80 025 Amiens Cedex 1, France

## ARTICLE INFO

### Keywords:

Straw bale house  
Straw bale wall  
U-value  
Hygrothermal performance  
Thermal inertia  
Moisture content

## ABSTRACT

This paper focuses on the assessment of the hygrothermal performance of a straw bale house in the Picardie, a region of France. The house was built using a wooden load bearing frame filled with straw bales. Laboratory and in situ tests were carried out in this study.

In the first part, the thermal conductivity of straw bales was measured in relation to the orientation of the straw fibers. The thermal resistance of a wall built in the laboratory, respecting the real construction parameters, was assessed. The obtained U-value was compared to those of different walls used in civil field engineering.

The second part of this paper continues with an assessment of the hygrothermal performance of a real straw bale house. Temperature and relative humidity measurements were recorded during more than one year, using sensors that were placed in indoors and outdoors, and at various depths of the walls and floors.

Finally, this paper is completed by a dynamic thermal simulation of the house, based on experimental laboratory investigations. During winter the simulated heating requirements are estimated at 59 kW h/m<sup>2</sup>. Moreover, the simulation under summer conditions shows the major influence of the building envelope on the thermal comfort. Thus, straw bale walls seems to provide significant thermal inertia in summer.

## 1. Introduction

The energy costs of construction and the impacts of building materials on the environment are at the core of social concerns, both for the manufacture of building materials, and for the construction and use of these buildings. This has led to renewed interest in traditional structures, which have historically been rejected by investors since the Second World War. Moreover, these kinds of structures promote renewable materials like straw. In France, the first straw-based construction was built in 1921 [1] and, over recent years, some studies [2–5] have been carried out to overcome the drawbacks linked to the use of straw in the construction field.

Straw was used in building throughout the 20th century and, in the last ten years, the advantages of this material have been recognized, such as great thermal and acoustic insulation, an energy efficient manufacturing process, and the decrease in carbon dioxide in the atmosphere due to the photosynthesis of straw [6,7]. This natural material grows by photosynthesis using solar energy, during a period from six months to one year. It is produced in large quantities and in many regions of the world. Straw is cheap and plentiful.

Straw bale-based buildings represent low energy consumption, durability and attractiveness, and it can be resistant to various attacks

thanks to a good choice of the building system [8]. The measurements of temperature and relative humidity in a straw bale house located in Bavaria, Germany [8] showed that the straw walls had excellent properties to provide excellent living conditions.

Straw is an organic material, intrinsically flammable, which can contain some proteins and carbohydrates leading to a decrease in sustainability [9]. Lastly, straw presents weak mechanical properties in compression, in bending and in stiffness [10–12]. The sustainability of straw-based buildings depends strongly on temperature, moisture, and a combination of both [13]. There are concerns regarding the long term effects of moisture on the durability of these materials in a temperate maritime climate such as the United Kingdom [7,9]. According to Steen et al. [14], a moisture content close to 20% (or a relative humidity of 70% RH) corresponds to the level at which biological activity begins. Moreover, straw bale walls can deteriorate due to various factors like building design or construction details. Temperature and moisture are essential parameters resulting from environmental factors linked to the site of implantation (orientation of walls, regional climate, etc.). Thus, this study focuses on laboratory and in situ investigations of these essential parameters, resulting from the moderate climate of the Picardie region of France.

The first part of this article focuses on the evaluation of the steady-

\* Corresponding author.

E-mail address: [omar.douzane@u-picardie.fr](mailto:omar.douzane@u-picardie.fr) (O. Douzane).

state thermal conductivity of straw bales, depending on the orientations of the straw fibers. Then, a load-bearing wall was manufactured in the laboratory with the same construction details as the full-size building. Few studies have involved the characterization of straw bale walls at the laboratory scale (Hot Box apparatus) [15–18] and this work proposes investigations on a full-scale straw bale wall, respecting the construction details. In the second part, sensors installed during the construction phase enable the building to be monitored. Temperature and moisture were recorded during one year at various places in the structure. Finally, a simulation based on laboratory investigations was used to assess the heating power requirements of the real house.

## 2. Laboratory investigations

### 2.1. Characterization of the thermal conductivity of straw bale

A guarded hot plate apparatus (GHP) was used to evaluate the thermal conductivity of straw bales according to the standard ISO 8302 [19]. Samples were prepared by cutting off straw bales to dimensions  $50 \times 50 \times 10 \text{ cm}^3$ . These straw bales were the same as those used to build the laboratory wall and the real house. The samples were placed in a polystyrene frame to facilitate handling. Two kinds of samples were prepared in relation to the orientation of the straw fibers. Samples were oven dried at  $65 \text{ }^\circ\text{C}$  to obtain a constant mass. The average of the density of the straw bales was  $80 \text{ kg/m}^3$ .

The guarded hot plate apparatus TAURUS, TLP 500-X1, enabled the measurement of the thermal conductivity of a sample at various temperatures between  $10 \text{ }^\circ\text{C}$  and  $40 \text{ }^\circ\text{C}$  with a step of  $10 \text{ }^\circ\text{C}$ , in steady-state conditions. The sample was placed between hot and cold plates, which were maintained at given constant temperatures. The plates were in perfect thermal contact with the specimen thanks to the application of a thermal grease. The ring guard heater ensured unidirectional heat flow through the sample. The measurement was made on the central heater of dimensions  $25 \times 25 \text{ cm}^2$ .

The results are presented in Fig. 1. A linear evolution of the thermal conductivity against mean temperature was obtained. For solid materials, thermal conductivity can be modeled by the following expression in steady-state conditions:

$$\lambda = \lambda_0(1 + a\theta) \quad (1)$$

where  $\lambda_0$  is the thermal conductivity of the solid at  $0 \text{ }^\circ\text{C}$ ,  $\theta$  is the mean temperature, and  $a$  is an experimental intrinsic property of the material. Table 1 summarizes the characteristics of straw depending on the orientation of the fibers, which were parallel or perpendicular to the heat flow.

The average value of dry thermal conductivity at  $10 \text{ }^\circ\text{C}$  ( $\lambda_{10 \text{ dry}}$ ) was  $0.0723 \pm 0.0014 \text{ W/(m.K)}$  and  $0.0510 \pm 0.0010 \text{ W/(m.K)}$  in the parallel and perpendicular orientations, respectively. This results are consistent with the literature, considering approximately the same density of straw bales [2].

### 2.2. Measurement of the U-value of a straw bale-based wall

Considering the high thermal efficiency and the weak mechanical properties of straw, a load-bearing structure combining straw bales and wooden frames is of great interest. The analysis of the whole straw bale-based wall, with a wooden frames, is an essential step in the characterization of this kind of construction. In fact, wooden frames, joints and plasters (lime plaster and/or plasterboard) seem to modify significantly the thermal resistance of the wall, compared to straw bales only.

A straw bale wall was manufactured in the laboratory, following the same design as the full-sized construction. The first step consisted of the assembly of the wooden frame. This was constituted by timber studs and header and bottom plates, with a cross-section of

$345 \times 45 \text{ mm}^2$ . Using a manual jack, some compressed straw bales, of  $40 \text{ mm}$  in thickness, were placed between the timber studs, which were spaced  $800 \text{ mm}$  from each others. Then, after planning the straw bales, some furring strips were fixed on the inner side to support  $13 \text{ mm}$  thickness plasterboard. On the outer side, a lime plaster was applied directly on the straw bales (average thickness of  $35 \text{ mm}$ ). Fig. 2 shows the construction details of the straw bale-based wall. The final average thickness of the wall was about  $520 \text{ mm}$ . Temperature and heat flow were recorded with type-T thermocouples and surface heat flowmeters  $500 \text{ mm}$  in length, which were placed on both side of the wall.

The straw bale wall was positioned between two climate chambers, as shown in Fig. 3. These chambers, regulated in temperature, enable the measurements of the thermal resistance of a variable thickness wall.

First, the temperature was maintained constant in the two climate chambers at  $18 \text{ }^\circ\text{C}$ , which represents an average indoor temperature. When the temperature had stabilized in the whole wall, a thermal solicitation was applied on the outer side of the wall by imposing a temperature of  $30 \text{ }^\circ\text{C}$ . The evolution of the superficial temperature and surface heat flow are shown in Fig. 4. The outdoor temperature is stabilized after approximately  $15 \text{ h}$  while the heat flow measured on both sides proved that the steady state was reached after  $20 \text{ h}$  of the test. The stabilized indoor temperature confirmed the assumption of Fourier's model for the estimation of the thermal resistance of the wall. The thermal resistance is calculated by the Fourier's law for a mono-directional heat flow in steady-state conditions:

$$R = \frac{\Delta T}{\phi} \quad (2)$$

where  $R$  is the thermal resistance,  $\Delta T$  is the temperature gradient between indoors and outdoors and  $\phi$  is the heat flow.

The analysis of the measured data led to a steady-state thermal resistance of  $4.86 \pm 0.37 \text{ m}^2\text{K/W}$ , or a  $U$ -value close to  $0.20 \pm 0.016 \text{ W/m}^2\text{K}$ . This  $U$ -value was determined as soon as the discrepancy between the indoor and outdoor heat flows was near 0 (20th hour of the test). This experimental result was compared to the thermal resistance of different walls commonly used in the building (see Fig. 5). Traditionally, reinforced concrete and concrete blocks are the two building systems most used in the construction field. These systems were finished with an insulation of  $100 \text{ mm}$  polystyrene (PS) and  $13 \text{ mm}$  plasterboard. Three other thermally-efficient building systems were studied: a cellular concrete brick ( $365 \text{ mm}$ ), a monomur brick ( $375 \text{ mm}$ ) with thin joints and a hemp concrete brick ( $300 \text{ mm}$ ). These bricks were finished with lime plaster on both sides and an indoor finishing composed of an air space and a plasterboard ( $13 \text{ mm}$ )

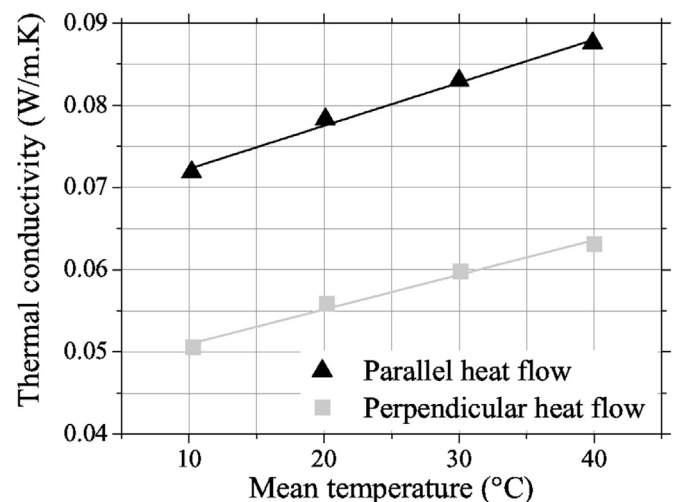


Fig. 1. Thermal conductivity of straw against mean temperature.

**Table 1**  
Intrinsic thermal properties of straw.

	$\lambda_0$ (W/(m.K))	$a$ (W/m)
Fibers parallel to heat flow	0.067	0.0078
Fibers perpendicular to heat flow	0.046	0.0090

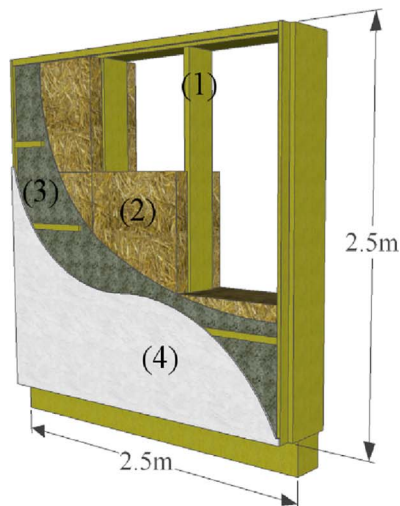
[20–22]. More information can also be found in [23].

In order to compare with different wall configurations which are largely used in France for building construction, two groups of wall building systems can be established as shown in Fig. 5. The first group includes the traditional load-bearing structures (reinforced concrete and concrete blocks) with a polystyrene insulation, with  $U$ -values around  $0.35 \text{ W}/(\text{m}^2.\text{K})$ . The second group includes building systems assuring the load-bearing capacity and thermal self-insulation, with  $U$ -values ranging from  $0.20$  to  $0.24 \text{ W}/(\text{m}^2.\text{K})$  (cellular concrete, hemp concrete and straw bales). These systems display high thermal properties compared to concrete, with a decrease in the  $U$ -value of up to 25%. Nevertheless, the results obtained for cellular concrete bricks and hemp concrete bricks must be viewed with caution because these results are based on their intrinsic thermal conductivity. In fact, the conductivity, obtained from suppliers, is an intrinsic values and does not take into consideration the whole load-bearing construction system, especially the joints between bricks. For example, the load-bearing wooden framework of the straw bale wall leads to an increase in the  $U$ -value close to 25%, compared to the designed  $U$ -value based on the conductivity of only straw bales, air space and plasterboard. Thus, the wooden framework, like joints between bricks, leads to a decrease in thermal efficiency. This comparison highlights the possibility of using renewable materials to meet current standards, with a  $U$ -value of  $0.25 \text{ W}/(\text{m}^2.\text{K})$  or less.

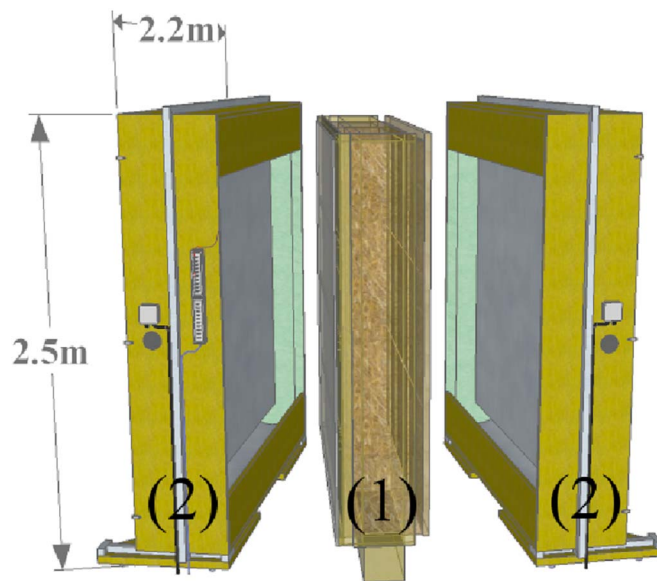
The  $U$ -value depends strongly on the thickness of the wall. For this reason, the use of apparent thermal conductivity is proposed so that the efficiency of walls can be compared. As an increase in the thickness of a wall leads to an increase in its thermal properties, the apparent thermal conductivity  $\lambda_{app}$  corresponds to the  $U$ -value multiplied by the thickness of the wall  $e$ :

$$\lambda_{app} = U \times e \tag{3}$$

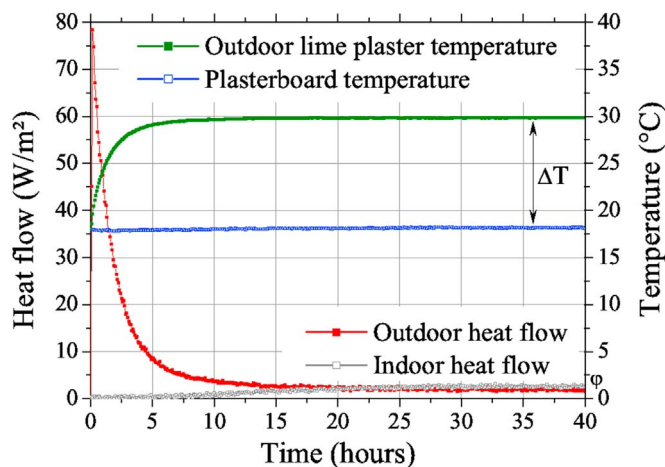
The apparent thermal conductivity of walls was estimated from the results presented in Fig. 5 and the findings are summarized in Table 2. Concrete and monomur brick present an apparent thermal conductivity close to  $0.13 \text{ W}/(\text{m.K})$  while the straw bale wall and cellular concrete show an apparent thermal conductivity close to  $0.10 \text{ W}/(\text{m.K})$ . Finally, the most efficient material is hemp concrete with an apparent thermal



**Fig. 2.** Construction details of the straw bale wall specimen: (1) wooden frame; (2) straw bales; (3) lime plaster; (4) plasterboard.

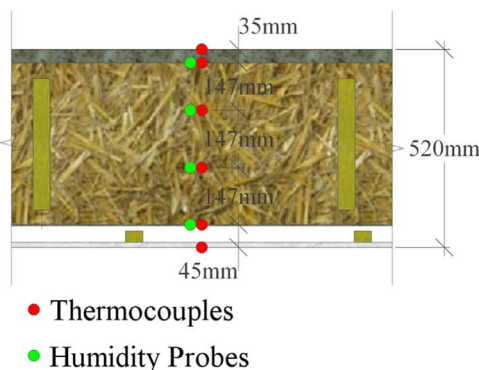


**Fig. 3.** Experimental setup for  $U$ -value measurement. Climate chambers (2) are placed on both sides of the straw bale wall (1).



**Fig. 4.** Evolution of heat flow and superficial temperature on the both sides of the straw bale wall.

conductivity of  $0.07 \text{ W}/(\text{m.K})$ . Nevertheless, all these results must be





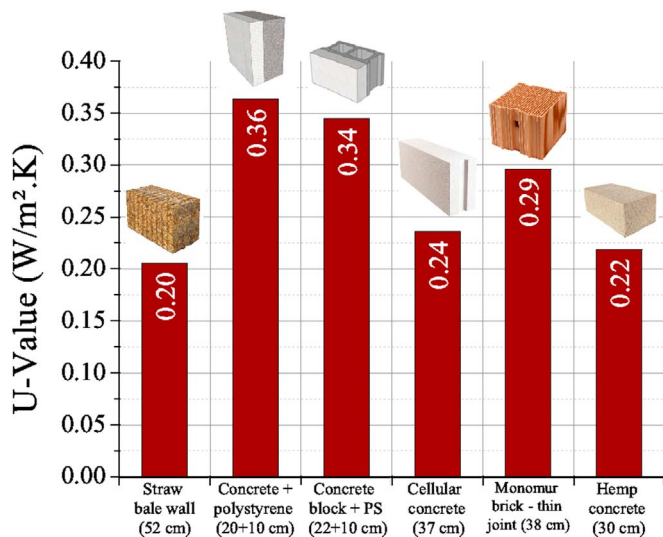


Fig. 5. Comparison of U-values for different wall specimens [9,18,20].

Table 2

Comparison of apparent thermal conductivity for different wall specimens.

Wall	$\lambda_{app}$ (W/(m.K))
Straw bale wall	0.104
Concrete+polystyrene	0.108
Concrete block+polystyrene	0.108
Cellular concrete	0.089
Monomur brick	0.110
Hemp concrete	0.066

viewed with cautions because apparent thermal conductivity is based on the intrinsic thermal conductivity of the bulk materials, excepted for the straw bale wall. The apparent thermal conductivity of the straw bale wall enabled the simulation of the heating requirements presented in the last part of this paper.

### 3. In situ investigations of the thermal and hygric performance of straw bale walls

This study focuses mainly on the thermal and hygric performance of a traditional straw bale building built in Voyennes (Picardie region) in the north of France. Fig. 6 presents the house, which is composed of a ground floor (divided into an open-plan kitchen/living room, a bedroom, a storeroom and a laundry room), and an upper floor with three bedrooms. The area of the house is approximately 188 m<sup>2</sup>.

The walls and floor were designed and constructed with a wooden load-bearing frame completed by straw bales, which were protected from detrimental weather conditions by an external layer of 4 cm-thick lime plaster. The whole structure of the walls is described in Section 2.2 above. The weather in Picardie is considered temperate, as it can be seen in Fig. 7.

Fig. 7 shows the evolution of the indoor and outdoor temperature and relative humidity during a period of 400 days, from the 25th May. Despite some fluctuations in the outdoor temperature, which reached almost 40 °C in summer and -10 °C in winter, the indoor temperature was relatively stable, around 20–25 °C, whatever the season. The indoor relative humidity (RH) was quite stable too, around 40–60% RH, despite the marked fluctuations in outdoor relative humidity linked to the climatic variations. In winter (day 190 corresponds to the 1st January), the outdoor relative humidity was quite high while the indoor relative humidity was very low (around 30–40%RH). This can be explained by the heating of the house which led to drier ambient air.

In order to assess the thermal and hygric performances of the straw bale house, temperature and relative humidity measurements were recorded at 38 points of the house. 28 type-T thermocouples and 10 HMP60 humidity probes were placed indoors and outdoors, and at various depths of northern/southern and ground floor/first floor walls and floors. The plans of this building show the location of the sensors (see Fig. 8). Temperature and relative humidity readings were recorded at 10 min intervals for a period of 14 months (from 25th May to 11th August).

#### 3.1. Evaluating thermal and hygric performances of the building envelope

To assess the hygrothermal performance of straw bale walls, temperature and relative humidity were measured on the internal and external sides of the south- and north-facing walls. Fig. 9 presents the evolution of the superficial temperature and humidity level on the internal and external sides of the south-facing wall on the ground floor. Despite the external temperature fluctuations, the internal temperature was quite stable, around 20 °C. These results show that the building envelope can be used to control the external peaks of temperature and thus lead to a better indoor comfort.

Moreover Fig. 9 shows large variations in relative humidity on the external side of the wall. These variations did not seem to have a significant impact on the internal relative humidity, which varied from 40% to 60%. Nevertheless, an occasional decrease of approximately 30% can occur during the winter period. This can be explained by the heating of the house, which led to a drier ambient air.

To prove the major influence of the straw bale wall on assuring the thermal comfort, especially during the summer period [24], Fig. 10 shows the evolution of the internal and external superficial temperatures for the south-facing wall. On 18th April, the magnitude of variation of the external temperature (which was higher than 25 °C) was barely noticeable on the internal side of the wall, with a maximal gap between the highest and the lowest values of about 3 °C, despite the lack of air conditioning. The two parameters of thermal inertia (damping rate and phase shift) are represented in Fig. 10. Damping rate  $\zeta$  is obtained from the following expression:

$$\zeta = \frac{\Delta T_{in}}{\Delta T_{out}} \quad (4)$$

where  $\Delta T_{in}$  and  $\Delta T_{out}$  are the temperature gradient indoors and outdoors, respectively. A phase shift of approximately 6 h and a heat flow damping rate of about 9% are highlighted. Due to the thermal inertia of the straw bale wall, the temperature peak recorded on the internal side was reached during the decrease in external temperature, especially during the night. This phenomenon limits overheating in summer.



Fig. 6. The straw bale house.

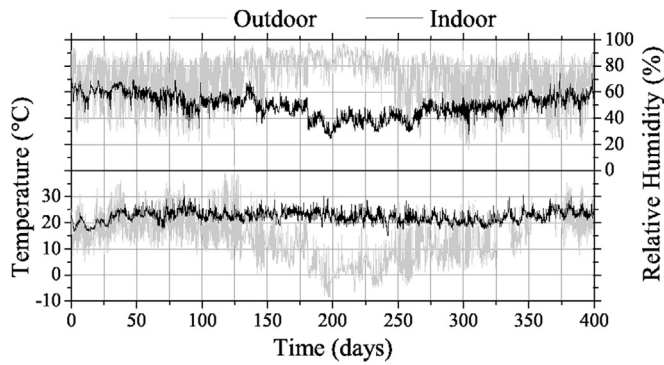


Fig. 7. Evolution of the indoor and outdoor temperatures and relative humidity for the studied building.

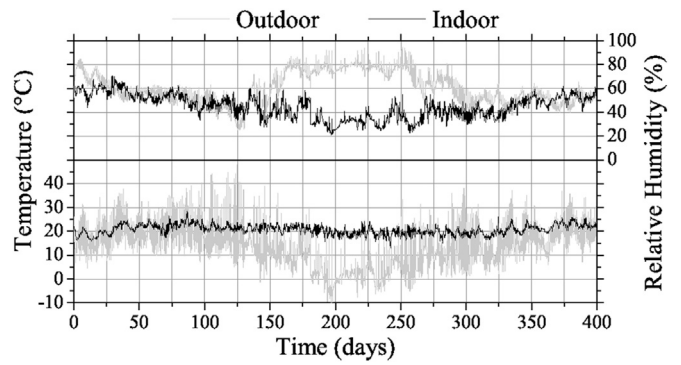


Fig. 9. Evolution of the external and internal superficial temperature and relative humidity.

### 3.2. Overheating range – summer comfort

In recent years, the concept of summer comfort has been approached by Brager [25,26] and Humphreys [27]. To define the comfort, these authors proposed to limit the indoor comfort temperature of a place as a function of the mean daily outdoor effective temperature varying between 10 °C and 34 °C. Expressions 5 and 6 present the comfort temperature  $T_{comf}$  depending on the mean outdoor temperature  $T_{m,out}$  for the adaptive models of Brager and Humphreys, respectively.

$$T_{comf} = 0.31 \times T_{m,out} + 17.8 \quad (5)$$

$$T_{comf} = 0.534 \times T_{m,out} + 11.9 \quad (6)$$

The feeling of comfort strongly depends on the occupant and thus can not be interpreted by mathematical indicators. In the light of this fact, Brager's adaptive model is completed by a qualitative approach of the satisfaction level of the occupant: a comfort range of 5 °C corresponds to a satisfactory rate of 90% while a 7 °C range translate into an 80% satisfactory rate (see Fig. 11). For all these reasons, Brager's model is used here to define the overheating range during the summer period.

The data collected during two summer periods (from 1st June to 31th August) are superimposed on the Brager chart. These experimental results were recorded in the living room on the ground floor,

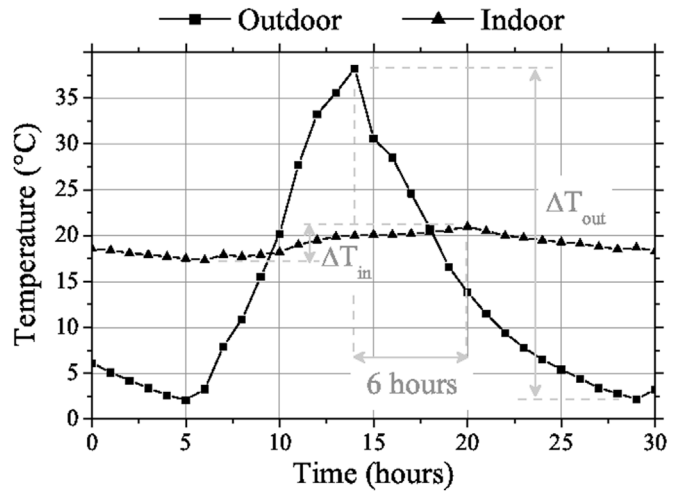


Fig. 10. Evolution of external and internal superficial temperature: detail on the 18th April.

which is south-facing. Here, the heat radiation was significant and led to an increased heat transfer over the wall. Nevertheless, Fig. 11 shows that indoor temperatures were mostly in the comfort range prescribed by Brager. Some experimental points were slightly below this comfort

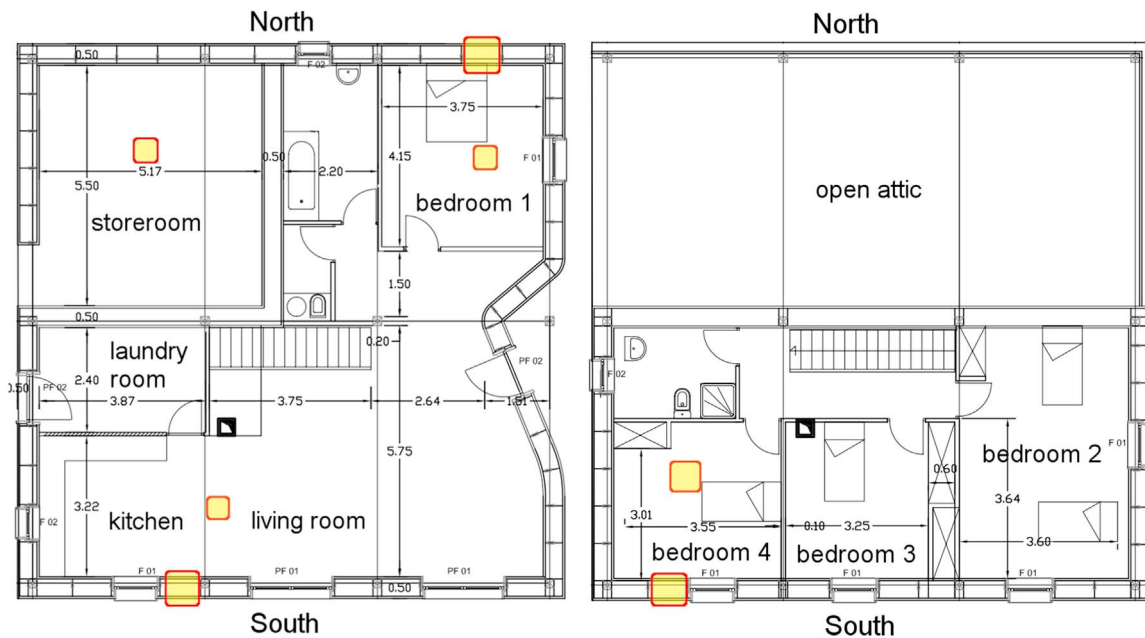


Fig. 8. Location of temperature and relative humidity sensors in the house.

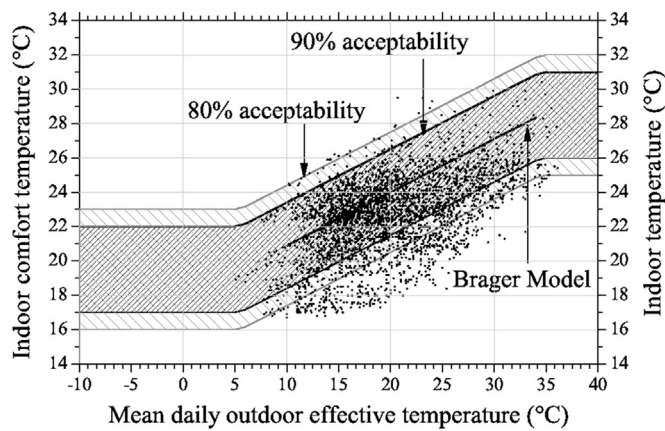


Fig. 11. Restricted comfort range prescribed by Brager as a function of the acceptability level.

range, leading to a discomfort level near 22% and 30% for a satisfaction level of 80% and 90% respectively. Only a few points were in the overheating range thus thermal comfort seems to be ensured by the straw bale envelope. This observation tends to confirm the influence of phase shift and damping of straw bale walls. The wall restored the daily stored heat with a phase shift of approx. 6 h, when the outdoor temperature was falling. The straw bale envelope seems to present a good thermal inertia.

### 3.3. Hygrothermal comfort diagram

The concept of comfort can not be limited to temperature only. It is commonly accepted that relative humidity has a significant impact on feeling comfortable. To this end, Fauconnier [28] proposed a model that defined a hygrothermal comfort range, characterizing the couple (temperature; humidity) required to feel comfortable. A combination of the Brager and Fauconnier models seems very relevant to define the hygrothermal comfort as a function of the outdoor temperature. This is presented in Fig. 12. This spatial representation of the comfort is based on the thermal comfort range prescribed by Brager, which is extruded following the orthogonal direction in relation of the hydric comfort introduced by Fauconnier.

Fig. 12 shows the same experimental points as those presented previously. The influence of relative humidity is significant regarding the hygrothermal comfort level. All recorded points out of the comfort range are drawn in red in the Fig. 12. For a 90% satisfactory level, the discomfort level rises to 32% with 74 new discomfort points recorded, compared to thermal discomfort. Moreover, with an 80% satisfactory rate, the hygrothermal discomfort reaches 25%. Finally, during these summer periods, when no heating power was required, the thermal resistance of the straw bale house led to the damping of the external temperature. The daily stored heat was restored during the night, through the phase shift. The summer thermal comfort was very good with no overheatings; just a very small number of points under the Brager range are highlighted by the chart.

### 3.4. Temperature and humidity profile in walls

Although indoor hygrothermal comfort is assured, the straw bale house needs to be monitored regarding the appearance and proliferation of mold inside the straw bales. Mold can appear when the relative humidity exceeds 85%. Thus, humidity profile and condensation risk analyses are necessary in straw bale walls. To achieve this, six temperature and moisture probes were placed in the south- and north-facing walls, at various depths. Only the data recorded in the north-facing ground floor wall is presented here because it showed the highest level of relative and absolute moisture. Moreover, north-facing

walls are less influenced by heat radiation. Unfortunately, a temperature sensor placed in the middle of the straw bale was faulty. Fig. 13 presents the temperature and moisture profiles in the north-facing wall. The relative moisture was always less than 100% inside the wall, which tends to confirm the lack of condensation inside the straw bales. Moreover, the influence of the lime plaster was clearly highlighted by the fall in relative humidity (more than 20%) in the depth of the coating. The decrease in relative moisture through the depth of the straw bale was linear and reached approximately 40%. The last centimeters corresponded to air space and plasterboard, which tended to regulate the indoor relative humidity.

Finally, no mold problem seemed to reduce the health comfort of the straw bale house (RH was always under 80%). In fact, the analysis of relative profiles proved the lack of condensation inside the wall. The influence of the coating is essential to reduce significantly the humidity inside the straw. Plasterboard seems to allow a hydric regulation of the ambient air.

It should be noted that the straw bale is a hygroscopic material, which means that it can absorb or release the moisture from the surrounding air. Fig. 14 shows the relative humidity distribution in the wall as a function of depth during one year. This provides an overview of the moisture behavior of layers of different materials during changing climate conditions. One can see from this figure that, due to the very high relative humidity of the outside air in winter, the humidity in the lime plaster was very high (with the maximum value up to 95% RH) while it was greatly reduced inside the straw bales (maximum value was 82% RH).

Within this study, it can be seen that the relative humidity in straw bales fluctuated between 25% and 82% RH. The moisture content can also be determined from the relative humidity measured using the sorption isotherm data. According to the data presented in [9], a relative humidity of 82% equals approximately to 19,5% of moisture content, which is still less than 20% moisture content at which most organic material, such as straw, starts to degrade [29].

## 4. Simulation of the thermal behavior

A simulation of the thermal behavior of the straw bale house, under dynamic conditions, was carried out using the “Pleiades+Comfie” software [30]. This numerical study assessed the heating requirements and discomfort periods, which were linked to overheating in the summer period.

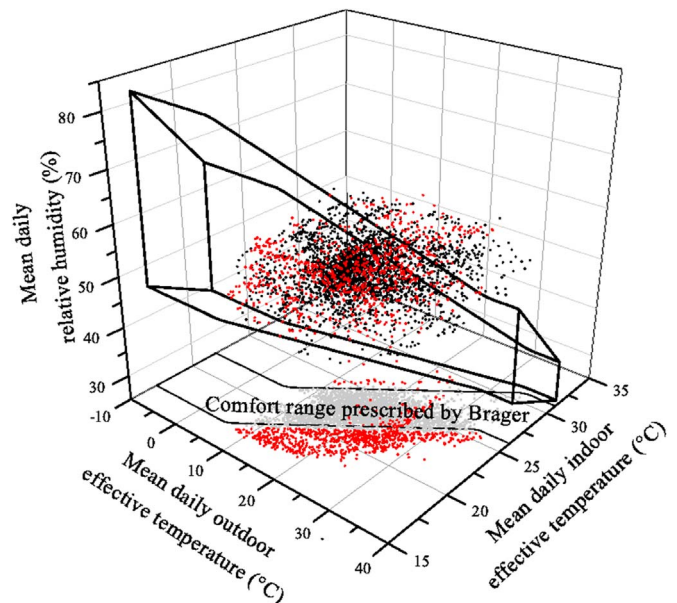


Fig. 12. Diagram of hygrothermal comfort.



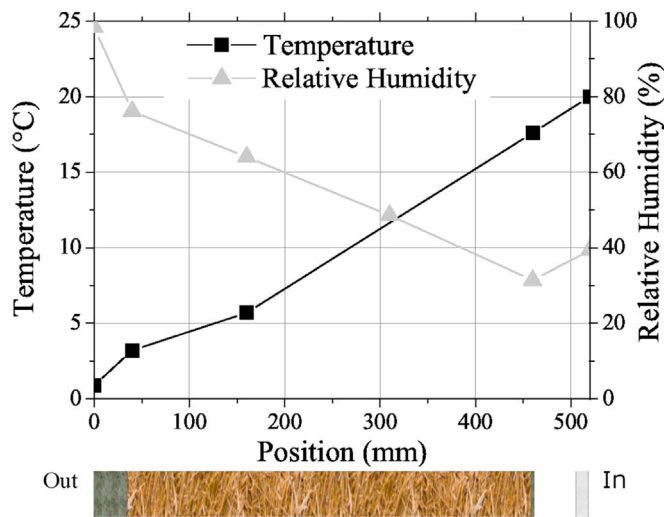


Fig. 13. Profile of temperature and relative moisture in the north-facing wall.

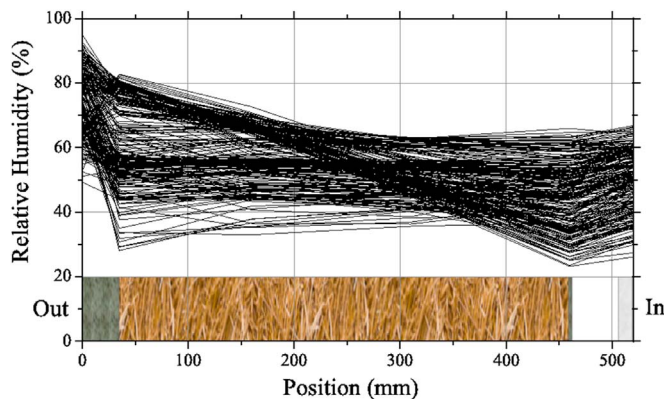


Fig. 14. Relative humidity distribution in the wall against depth.

Table 3  
Simulated heating power.

	Heating power	Heating power per m <sup>2</sup>	Power consumption	Solar gains	Heat losses
	(kW h)	(kW h)	(W)	(kW h)	(kW h)
Bedroom 1	1 355	59	1 779	1 364	1 697
Bathroom 1	723	56	1 295	61	841
Bathroom 2	562	53	826	0	627
Bedrooms 2, 3, 4	3 870	51	5617	778	5 372
Kitchen/living room	4 581	54	7 315	1 804	7 883
Total	11,091	59	16,833	2 777	16,420

The simulation assumptions were the following ones: the apparent thermal conductivity of walls and floors are 0.107 W/(m.K) and the specific heat capacity is 490 kJ/(m<sup>3</sup>.K). The apparent thermal conductivity value was obtained from experimental investigation from laboratory tests on the straw bale wall. The thermal bridge corresponds to self-insulation. The air flow rate is compliant with the health and safety policy (30 m<sup>3</sup>/h for a bedroom and 105 m<sup>3</sup>/h for the kitchen/living room). Air permeability of the house is considered equal to 1.3 m<sup>3</sup>/h, the minimal value required by the French standard RT2005. Finally, a medium exposure to wind class is taken into account. Air infiltration was calculated by the standard EN 13790 [31] regarding the thermal performance of buildings. This leads to an air change rate of 0.59 vol/h for the whole house. Concerning internal heat gains, a five person family is considered.

Table 4  
Summer overheating and discomfort level.

	Solar Gains (kWh)	Overheating (°C)	Outdoor T Amplification (%)	Discomfort Level (%)
Storeroom	0	0	2.16	0
Bedroom 1	75	0	13.53	0
Bathroom 1	34	0	11.77	0
Laundry room	0	0	14.68	0
Bathroom 1	0	0.13	16.94	0
Bedrooms 2, 3, 4	294	0.89	23.63	0
Kitchen/living room	614	0.96	28.40	6.84
Total	1 017			

#### 4.1. Simulation during the winter period

The building is assumed to be fitted with a regulated heating equipment that keeps the indoor temperature at around 18 °C during the day and 15 °C during the night. Table 2 summarizes the detailed results. The heat losses are assessed at about 16,420 kW h during the whole heating period. 17% of these are covered by the solar gains received. Thus, the heating requirements are equal to 11,091 kW h, or 59 kW h. The maximal overall power consumption is about 16.8 kW. Table 3.

#### 4.2. Simulation during the summer period

The bedrooms located on the first floor and the kitchen/living room show some periods of overheating during summer. These are essentially between 0.9 °C and 1 °C. Considering a discomfort level when the temperature is higher than 27 °C, only the kitchen/living room is concerned (65%), because the bedrooms are not occupied during the day. Table 4 summarizes the results of this simulation.

The simulation of the indoor temperature in the kitchen/living room and in the first floor bedrooms shows that the magnitude of variation of the indoor temperature can reach 4 °C, despite the higher magnitude of variation of the outdoor temperature (maximum of 13 °C). The thermal comfort, prescribed by Brager, gives a very satisfactory level. The building envelope can reduce strongly the daily indoor temperature variations due to the outdoor meteorological variations and thus preserves the thermal comfort of the occupants.

### 5. Conclusion

This study provides an in situ analysis of the hygrothermal performance of a straw bale house built in Picardie (France). The experimental study was completed by laboratory investigations. The measurement of thermal conductivity of straw bales (as function of the orientation of the straw fibers), as well as the assessment of thermal resistance of a straw bale wall similar to those constructed for the real house showed the insulation power of this bio-based material.

In situ measurements of temperatures and relative humidity showed the hygrothermal performance of the building envelope. The temperature and humidity profiles, recorded at various depths of walls (north- and south-facing), revealed that there was no condensation risk in the straw bale walls. In addition, the influence of the limeplaster coating on the protection of straw against mold appearing at a high moisture content was highlighted. The indoor temperature and relative humidity recorded showed that the material can provide excellent living conditions which have been confirmed by the occupants.

A dynamic simulation of the thermal behavior of the straw bale building, based on experimental results measured in laboratory, has

been carried out. The numerical results confirmed that using straw bale material can ensure a good thermal performance and a high thermal comfort.

### Acknowledgments

The authors are very grateful to the Picardy Region and the French Environment and Energy Management Agency (ADEME) for supporting this work. Moreover, we would like to thank M. Champain, architect of the Vivarchi company, for his collaboration and his expertise.

### References

- [1] O.Krumm and E.Cauderay, La construction en botte de paille. Etude de faisabilité, ([www.atba.ch/articles/Etude2.pdf](http://www.atba.ch/articles/Etude2.pdf)), (accessed on 28.04.16), 2009.
- [2] A.Grelat, Utilisation de la paille en parois de maisons individuelles à ossature bois. Extrait du rapport final, Tome 2, Expérimentations en laboratoires et instrumentation in-situ, CEBTP/ADEME, 2004.
- [3] J. Wihan, Humidity in straw bale walls and its effect on the decomposition of straw (PhD thesis), University of East London School of Computing and Technology, London, United Kingdom, 2007.
- [4] S.T. Elias-Ozkan, F. Summers, N. Surmeli, S. Yannas, A comparative study of the thermal performance of building materials, in: Proceedings of the 23rd Conference on Passive and Low Energy Architecture. PLEA 2006, 6–8 September, 2006.
- [5] S.T. Elias-Ozkan, F. Summers, T. Karaguzel, O. Taner, Analyzing environmental performance of AAC blocks, strawbales and mud-plaster in hybrid wall construction, in: Proceedings of the 25th Conference on Passive and Low Energy Architecture. PLEA 2008, 22–24 October, 2008.
- [6] D.A. Bainbridge, Houses of straw: building solid and environmentally conscious foundations, *Eng. Technol. Sustain. World* 12 (4) (2005) 7–8.
- [7] J. Carfrae, P. De Wilde, J. Littlewood, S. Goodhew, P. Walker, Development of a cost effective probe for the long term monitoring of straw bale buildings, *Build. Environ.* 46 (2011) 156–164.
- [8] T. Ashour, H. Georg, W. Wu, Performance of straw bale wall: a case of study, *Energy Build.* 43 (2011) 1960–1967.
- [9] M. Lawrence, A. Heath, P. Walker, Determining moisture levels in straw bale construction, *Constr. Build. Mater.* 23 (2009) 2763–2768.
- [10] T. Ashour, H. Wieland, H. Georg, F.J. Bockisch, W. Wu, The influence of natural reinforcement fibres on insulation values of earth plaster for straw bale buildings, *Mater. Des.* 31 (2010) 4676–4685.
- [11] M.A. Grandsaert. Compression test of plastered straw-bale walls, in: Proceedings of the First International Conference on Ecological Building Structure, San Rafael, 2001.
- [12] S. Vardy, C. MacDougall, Compressive testing and analysis of plastered straw bales, *J. Green. Build.* (2006).
- [13] T. Ashour, H. Georg, W. Wu, An experimental investigation on equilibrium moisture content of earth plaster with natural reinforcement fibers for straw bale buildings, *Appl. Therm. Eng.* 31 (2011) 293–303.
- [14] S. Goodhew, R. Griffiths, T. Woolley, An investigation of the moisture content in the walls of a straw-bale building, *Constr. Build. Mater.* 39 (2004) 1443–1451.
- [15] M. Qin, R. Belarbi, A. Ait-Mokhtar, L.-O. Nilsson, Coupled heat and moisture transfer in multi-layer building materials, *Constr. Build. Mater.* 23 (2009) 967–975.
- [16] M. Qin, A. Ait-Mokhtar, R. Belarbi, Two-dimensional hygrothermal transfer in porous building materials, *Appl. Therm. Eng.* 30 (2010) 2555–2562.
- [17] K. Ghazi Wakili, and Ch. Tanner. U-value of a dried wall made of perforated porous clay bricks. Hot box measurement versus numerical analysis, *Energy Build.* 35 (2003) 675–680.
- [18] T. Nussbaumer, K. Ghazi Wakili, and Ch. Tanner. Experimental and numerical investigation of the thermal performance of a protected vacuum-insulation system applied to a concrete wall, *Appl. Energy* 83 (2006) 841–855.
- [19] Norme ISO 8302, Isolation thermique - détermination de la résistance thermique et des propriétés connexes en régime stationnaire - méthode de la plaque chaude gardée, 1991
- [20] T.Imerys Cuite. ([www.imerys-structure.com/professionnels/cmi/default.asp](http://www.imerys-structure.com/professionnels/cmi/default.asp)) (accessed on 28.04.16).
- [21] Beton HL2R cellulaire. ([www.hl2r.fr/isolation-beton-cellulaire](http://www.hl2r.fr/isolation-beton-cellulaire)) (accessed on 28.04.16).
- [22] Chanvribloc. ([www.chanvribloc.com/chanvribloc-produits.html](http://www.chanvribloc.com/chanvribloc-produits.html)) (accessed on 28.04.16).
- [23] S. Goodhew, R. Griffiths, Sustainable earth walls to meet the building regulations, *Energy Build.* 37 (2005) 451–459.
- [24] E. Stephan, R. Cantin, A. Caucheteux, S. Tasca-Guernouti, P. Michel, Experimental assessment of thermal inertia in insulated and non-insulated old limestone buildings, *Build. Environ.* 80 (2014) 241–248.
- [25] R.J. De Dear, G.S. Brager, Developing an adaptive model to thermal comfort and preference, *ASHRAE Trans.* 104 (Part 1A) (1998) 145–167.
- [26] R.J. De Dear, G.S. Brager, Thermal comfort in naturally ventilated buildings: revisions to ASHRAE standard 55, *Energy Build.* 34 (6) (2002) 549–561.
- [27] M.A. Humphreys, F. Nicol, Understanding the adaptive approach to thermal comfort, *ASHARE Trans.* 104 (Part 1) (1998) 991–1004.
- [28] R. Fauconnier, L'action de l'humidité de l'air sur la santé dans les bâtiments tertiaires, *Rev. Chauff. Vent. Cond.* 10 (1992).
- [29] M.D. Summers, Moisture and decomposition in straw: implications for straw bale construction, in: B. King (Ed.) *Design of Straw Bale Buildings*, Green Building Press, San Rafael (CA), 2006, pp. 162–172.
- [30] T.Salomon, R.Mikolase, B.Peuportier, Tool for dynamic building thermal simulation, Comfie SFT-IBPSA, Software Pleaides – Comfie, 2005, Available from: Izuba Energies. (<http://www.izuba.fr;2011>)
- [31] EN ISO 13790:2008. Thermal performance of buildings - calculation of energy use for space heating and cooling. ISO, 2008.